

---

# Zero-Cost Proxies Meet Differentiable Architecture Search

---

Lichuan Xiang<sup>1†</sup>, Lukasz Dudziak<sup>2†</sup>, Mohamed S. Abdelfattah<sup>2†</sup>  
 Thomas Chau<sup>2</sup>, Nicholas D. Lane<sup>2,3</sup>, Hongkai Wen<sup>1,2\*</sup>

<sup>1</sup> University of Warwick, UK    <sup>2</sup> Samsung AI Center Cambridge, UK

<sup>3</sup> University of Cambridge, UK    <sup>†</sup>Indicates equal contributions

{l.xiang.2, hongkai.wen}@warwick.ac.uk

{l.dudziak, mohamed1.a, thomas.chau, nic.lane}@samsung.com

## Abstract

Differentiable neural architecture search (NAS) has attracted significant attention in recent years due to its ability to quickly discover promising architectures of deep neural networks even in very large search spaces. Despite its success, DARTS lacks robustness in certain cases, e.g. it may degenerate to trivial architectures with excessive parametric-free operations such as skip connection or random noise, leading to inferior performance. In particular, operation selection based on the magnitude of architectural parameters was recently proven to be fundamentally wrong showcasing the need to rethink this aspect. On the other hand, zero-cost proxies have been recently studied in the context of sample-based NAS showing promising results – speeding up the search process drastically in some cases but also failing on some of the large search spaces typical for differentiable NAS. In this work we propose a novel operation selection paradigm in the context of differentiable NAS which utilises zero-cost proxies. Our “perturbation-based zero-cost operation selection” (Zero-Cost-PT) improves searching time and, in many cases, accuracy compared to the best available differentiable architecture search, regardless of the search space size. Specifically, we are able to find comparable architectures to DARTS-PT on the DARTS CNN search space while being over  $40\times$  faster (total searching time 25 minutes on a single GPU). Our code will be available at: <https://github.com/avail-upon-acceptance>.

## 1 Introduction

Since the recent dawn of deep learning, researchers have been working on developing new architectures of neural networks on an unprecedented scale, with more efficient and accurate networks being proposed each year [1, 2, 3]. However, designing new architectures in order to push the frontier has proven to be a challenging task, requiring extensive domain knowledge and persistence in searching for the most optimal combination of hyperparameters [4, 5]. Recently this process has been successfully aided by the usage of automated methods, especially neural architecture search (NAS) which, at the moment of writing, can be found behind many of the state-of-the-art deep neural networks [6, 7, 8, 9].

However, one of the biggest problems in NAS is the computational cost – even training a single deep network can require enormous computational resources and many NAS methods need to train tens, if not hundreds, of networks in order to fully show their potential [6, 10, 11]. A related problem concerns search space size – often more available options mean that we can find a better combination, but it also means longer searching time [6]. Differentiable architecture search (DARTS) was first

---

\*Corresponding author.

proposed to tackle those challenges, showcasing promising results when searching for a network in a set of over  $10^{18}$  possible variations [12].

Unfortunately, DARTs has been proven to have some significant robustness issues [13, 14, 15]. It also requires careful selection of hyperparameters which makes it relatively hard to use on a new task. At the same time, sample-based NAS often does not exhibit those challenges although it requires orders of magnitude more computation. In order to reduce searching time during sample-based NAS, *proxies* are often used to obtain approximated performance of different models without the necessity of their full training (which is the main factor behind their expensive searching cost). Most recently, *zero-cost proxies* [16, 17], which are extreme types of NAS proxies that do not require any training, have gained interest and are shown to empirically deliver outstanding results on common NAS benchmarks [16]. However, their efficient usage in a much larger setting, typical for differentiable NAS, is much more challenging compared to what is commonly used in sample-based NAS and thus remains an open problem [17].

In this paper we combine the most recent advances in differentiable NAS and zero-cost proxies to further push the efficiency of NAS on very large search spaces.

## 2 Related work

**Classic NAS and Proxies.** Zoph & Lee were among the first to propose an automated method to search for a neural network’s structure [18]. In their paper, a reinforcement learning agent is optimised to maximise rewards coming from training of models with different architectures. Since then, a number of alternative approaches have been proposed in order to reduce the significant searching time introduced by the need to train each proposed model. Among those, Pham et al. proposed to train models using only one epoch but preserve weights between trainings [19] – an approach classified as *one-shot* method that is very close to the differentiable NAS described below [20, 21]. In general, reduced training (with or without weight sharing) can be found in many works using NAS [22]. Other popular proxies involve searching for a model on a smaller dataset and then transfer the architecture to the larger target dataset [6, 23] or incorporating a predictor into the search process [24, 11, 25, 26].

**Zero-cost Proxies.** Very recently, zero-cost proxies for NAS emerged from pruning-at-initialisation literature [17, 16]. Zero-cost proxies for NAS aim to score a network architecture at initialisation, which is hoped to have certain correlations with its final trained accuracy. The scores, indicating the “saliency” of the architecture, can be either used to substitute the expensive training step in traditional NAS, or better guide the exploration in existing NAS solutions. Such proxies can be formulated as architecture scoring functions  $S(A)$  that evaluate the potential of a given neural architecture  $A$  in achieving accuracy. In this paper, we adopt zero-cost proxies as in [16], namely `grad_norm`, `snip`, `grasp`, `synflow` and `fisher`. Those metrics draw heavily from the pruning-at-initialisation literature [27, 28, 29, 30] and aggregate the saliency of model parameters to compute the score of an architecture. In addition, we also consider the metric `nwo` introduced in [17], which uses the overlapping of activations between different samples within a minibatch of data as a performance indicator.

**Differentiable NAS.** Liu et al. first proposed to search for a neural network’s architecture by parameterizing it with continuous values (called architectural parameters) in a differentiable way and then optimising using:  $\nabla_\alpha \mathcal{L}_v(w - \xi \nabla_w \mathcal{L}_t(w, \alpha), \alpha)$  [12]. Their method achieved significant reduction in searching time, due to the fact that architectural parameters ( $\alpha$ ) are optimised together with a network’s parameters ( $w$ ) in the same process. However, to do that all candidate operations have to be present and have architectural parameters assigned to them in a single structure that is commonly called a *supernet*, that is, a network that is a superposition of all networks in a search space. In order to extract the final architecture from the supernet, after architectural parameters have converged, operations with the largest magnitudes of  $\alpha$  are preserved (it is assumed that higher  $\alpha$  means more important operation). Despite efficiency of DARTS in terms of searching time, its stability and generalizability have been challenged. For instance, Zela et al. pointed out that DARTS generates architectures which yield high validation accuracy during the search phase but perform poorly in the final evaluation, and that it favours architectures dominated by skip connections [13]. SDARTS [31] proposed to overcome the issues mentioned above by smoothing the loss landscape by either random smoothing or adversarial training. SGAS [32] alleviated the discrepancy between the search and evaluation phases by selecting and pruning candidate operations sequentially with a greedy algorithm, such that at the end of the search phase, a network without weight sharing is obtained and thus the validation accuracy reflects the final evaluation accuracy.

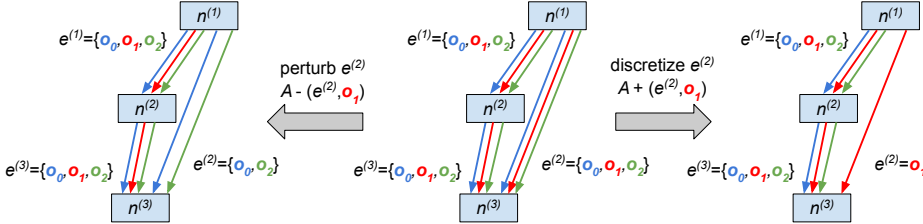


Figure 1: Visualisation of perturbation and discretization of an edge in a supernet.

**Perturbation-based NAS.** Recently, Wang et al. showed that the operation selection in DARTS based on the magnitude of  $\alpha$  is fundamentally wrong and proposed an alternative approach based on perturbations [33]. In this approach, the importance of operations is determined by the decrease of the super-network’s validation accuracy when an operation is removed (perturbation), and the most important operations are identified by exhaustively comparing them with other alternatives on a single edge of the super-network. Although their method uses a super-network as in DARTS, architecture selection is no longer performed by the means of derivative of structure-controlling parameters, formally it should not be put under the umbrella of differentiable NAS because operation selection occurs in a non-differentiable manner. However, it was proposed as a solution to problems specific to differentiable NAS, and to the best of our knowledge, is currently the only method in its category. Therefore, in the remaining parts of the paper we will consider perturbation-based algorithms to be a special case of differentiable methods.

### 3 Rethinking Operation Scoring in Differentiable NAS

In the context of differentiable architecture search, a supernet would contain multiple candidate operations on each edge as shown in Figure 1. Operation scoring functions assign a score to each operation out of the candidate operations – the operation with the best score is selected. In this section, we empirically quantify the effectiveness of existing operation scoring methods in differentiable NAS, with a specific focus on DARTS [12] and the recently-proposed DARTS-PT [33]. We challenge some of the assumptions made in previous work and show that, at least empirically, we can outperform existing operation scoring methods with a lightweight alternative based on zero-cost proxies [16].

#### 3.1 Operation Scoring Preliminaries

For a supernet  $A$  we want to be able to start *discretizing* edges in order to derive a subnetwork. When discretizing we replace an edge composed of multiple candidate operations and their respective (optional) architectural parameters  $\alpha$  with only one operation selected from the candidates. We will denote the process of discretization of an edge  $e$  with operation  $o$ , given a model  $A$ , as:  $A + (e, o)$ . Analogically, the *perturbation* of a supernet  $A$  by removing an operation  $o$  from an edge  $e$  will be denoted as  $A - (e, o)$ . Figure 1 illustrates discretization and perturbation.

NAS can then be performed by iterative discretization of edges in the supernet, yielding in the process a sequence of partially discretized architectures:  $A_0, A_1, \dots, A_{|\mathcal{E}|}$ , where  $A_0$  is the original supernet,  $A_{|\mathcal{E}|}$  is the final fully-discretized subnetwork (result of NAS), and  $A_t$  is  $A_{t-1}$  after discretizing a next edge, i.e.,  $A_t = A_{t-1} + (e_t, o_t)$  where  $t$  is an iteration counter.

The goal of operation scoring in this setting is to find the operation that maximizes the achievable accuracy for a given edge and its supernet at iteration  $t$  – let’s denote this function as  $f(A_t, e) : \mathcal{A} \times \mathcal{E} \rightarrow \mathcal{O}_e$ , where  $\mathcal{A}$  is the set of all possible variations of  $A$ ,  $\mathcal{E}$  is the set of edges in a supernet, and  $\mathcal{O}_e$  is the set of candidate operations for the edge  $e$ . Let  $\mathcal{A}_{|\mathcal{E}|}$  denote all possible fully-discretized subnetworks. Furthermore, let us denote the set of possible fully-discretized subnetworks  $A_{|\mathcal{E}|}$  derived from  $A_t + (e, o)$  at iteration  $t$  as  $\mathcal{A}_{t,e,o} \subset \mathcal{A}_{|\mathcal{E}|}$ . The optimal operation scoring function is:

$$f_{\text{best-acc}}(A_t, e) = \arg \max_{o \in \mathcal{O}_e} \max_{A_{|\mathcal{E}|} \in \mathcal{A}_{t,e,o}} V^*(A_{|\mathcal{E}|}) \quad (1)$$

where  $V^*$  is validation accuracy of a network after full training (we will use  $V$  to denote validation accuracy without training). It is easy to see that if  $f_{\text{best}}$  were to be used to discretize all edges in a supernet, it should yield the best model in the search space, regardless of the order in which edges are discretized. Because of this, we argue that this function is the ultimate target for operation scoring in supernet-based NAS.

Table 1: Model selected based on maximizing each operation strength independently.

	best-acc	avg-acc	disc-acc	darts-pt	zc-pt	disc-zc	darts
Avg. Error <sup>1</sup> [%]	5.63	6.24	13.55	19.43	5.81	22.96	45.7
Rank in NAS-Bench-201	1	166	12,744	13,770	14	14,274	15,231

<sup>1</sup> Computed as the average of all available seeds for the selected model in NAS-Bench-201 CIFAR-10 dataset.

It might be more practical to consider the expected achievable accuracy when an operation is selected, instead of the best. Therefore we also define the function  $f_{\text{avg}}$ :

$$f_{\text{avg-acc}}(A_t, e) = \arg \max_{o \in \mathcal{O}_e} \mathbb{E}_{A_{|\mathcal{E}|} \in \mathcal{A}_{t,e,o}} V^*(A_{|\mathcal{E}|}) \quad (2)$$

In practice, we are unable to use either of the two functions  $f_{\text{best-acc}}$  or  $f_{\text{avg-acc}}$ , since we would need to have the final validation accuracy  $V^*$  of all the networks in the search space. There have been many attempts at approximating the operation scoring functions, in the following we consider the following practical alternatives presented in DARTS [12] and DARTS-PT [33]:

$$f_{\text{darts}}(A_t, e) = \arg \max_{o \in \mathcal{O}_e} \alpha_{e,o} \quad (3)$$

$$f_{\text{disc-acc}}(A_t, e) = \arg \max_{o \in \mathcal{O}_e} V^*(A_t + (e, o)) \quad (4)$$

$$f_{\text{darts-pt}}(A_t, e) = \arg \min_{o \in \mathcal{O}_e} V(A_t - (e, o)) \quad (5)$$

where  $\alpha_{e,o}$  is the architectural parameter assigned to operation  $o$  on edge  $e$  as presented in darts [12].  $f_{\text{disc-acc}}$  is the accuracy of a supernet after an operation  $o$  is assigned to an edge  $e$  – this is referred to as “discretization accuracy” in the DARTS-PT paper and is assumed to be a good operation scoring function [33], most intuitively, it could approximate  $f_{\text{avg-acc}}$ .  $f_{\text{darts-pt}}$  is the perturbation-based approach used by DARTS-PT – it is presented as a practical and lightweight alternative  $f_{\text{disc-acc}}$  [33].

Similarly, we present the following scoring functions that use a zero-cost proxy  $S$  instead of validation accuracy when discretizing an edge or perturbing an operation. Note that the supernet is randomly-initialized and untrained in this case.

$$f_{\text{disc-zc}}(A_t, e) = \arg \max_{o \in \mathcal{O}_e} S(A_t + (e, o)) \quad (6)$$

$$f_{\text{zc-pt}}(A_t, e) = \arg \min_{o \in \mathcal{O}_e} S(A_t - (e, o)) \quad (7)$$

### 3.2 Empirical Evaluation of Operation Scoring Methods

In this subsection we investigate the performance of different operation scoring methods. Because we want to compare with the optimal  $f_{\text{best-acc}}$  and  $f_{\text{avg-acc}}$ , we conducted experiments on NAS-Bench-201 which contains the validation accuracy for all 15,625 subnetworks in their supernet search space [34].

We computed the operation score for all operations and all edges at the first iteration of NAS, that is,  $g(A_0, e, o)$ <sup>2</sup>  $\forall e \in \mathcal{E}, o \in \mathcal{O}_e$ . We then used these operation strengths to perform two experiments: The first experiment is shown in Figure 2. We plot the Spearman rank correlation coefficient of different scoring functions, averaged over all edges. In the second experiment, we use the operation scores  $g(A_0, e, o)$  to select the best operation according to that score. Note that this is precisely the NAS approach used in DARTS [12] where they check their operation score  $\alpha$  in one shot at the end of the supernet training. However, with the remaining methods, the operation score is



Figure 2: Spearman’s rank correlation coefficient of different operation scoring metrics with each other.

<sup>2</sup>Note that  $g(A_0, e, o)$  is simply  $f(A_0, e)$  without the  $\arg \min$  or  $\arg \max$  part.

---

**Algorithm 1:** Zero-Cost Perturbation-based Architecture Search (Zero-Cost-PT)

---

**Input :** An untrained supernet  $A_0$  with set of edges  $\mathcal{E}$ , # of search iterations  $N$ , # of validation iterations  $V$

**Result:** A selected architecture  $A_{|\mathcal{E}|}^*$

// Stage 1: search for architecture candidates

1  $\mathcal{C} = \emptyset$

2 **for**  $i = 1 : N$  **do**

3   **for**  $t = 1 : |\mathcal{E}|$  **do**

4     Select next edge  $e_t$  using the chosen discretization ordering

5      $o_t = f_{zc-pt}(A_{t-1}, e_t)$

6      $A_t = A_{t-1} + (e_t, o_t)$

7   **end**

8   Add  $A_{|\mathcal{E}|}$  to the set of candidate architectures  $\mathcal{C}$

9 **end**

// Stage 2: Validate the architecture candidates

10 **for**  $j = 1 : V$  **do**

11   Calculate  $S^{(j)}(A)$  for each  $A \in \mathcal{C}$  using a random mini-batch data;

12 **end**

13 Select the best architecture  $A_{|\mathcal{E}|}^* = \arg \max_{A \in \mathcal{C}} \sum_{j=1:V} S^{(j)}(A)$ ;

---

iteratively computed *after* each edge is discretized, potentially with additional training epochs in between iterations (as in the darts-pt and disc-acc metrics).

Figure 2 shows many surprising findings. First, disc-acc is inversely correlated to best-acc. This refutes the claim in the DARTS-PT paper that disc-acc is a reasonable operation score [33]. Our findings are aligned with prior work that has already shown that the supernet accuracy is unrelated to the final subnetwork accuracy [32]. Second, the darts-pt score does not track disc-acc, in fact, it is inversely-correlated to it as well. This means that the darts-pt score is not a good approximation of disc-acc. However, darts-pt is weakly-correlated to the “oracle” best-acc and avg-acc scores which could explain (empirically) why it works well. Third, zc-pt is strongly-correlated with both the best-acc and avg-acc metrics, indicating that there could be huge promise when using this scoring function within NAS. Note that disc-zc, like disc-acc is inversely correlated with our oracle score suggesting that perturbation is generally a better scoring paradigm than discretization. Finally, the original darts  $\alpha$  score is weakly and inversely correlated with the oracle scores, further supporting arguments in prior work that this is not an effective operation scoring method.

Table 1 shows which subnetwork is found when we use our seven operation scoring functions. As expected, best-acc chooses the best subnetwork from the NAS-Bench-201 supernet. avg-acc selects a very good model but not the best one, this is likely due to the large variance of accuracies in NAS-Bench-201. zc-pt selected one of the top models in NAS-Bench-201 as expected from the strong correlation with the oracle best-acc function. The remaining operation scoring functions failed to produce a good model in this experiment. This does not mean that these scores do not work in the general NAS setting in which operations are selected iteratively and with training in between iterations. However, our results suggest that these metrics do not make a good initial choice of operations at iteration 0. We take these results as an indication that existing operation scoring functions could be improved upon, especially using zc-pt which performed exceptionally well in our NAS-Bench-201 experiment.

## 4 Zero-Cost-PT Neural Architecture Search

In this section, we introduce our proposed NAS based on zero-cost perturbation, and we perform ablation studies to find the best set of heuristics for our search methodology, including: edge discretization order, number of search and validation iterations, and the choice of the zero-cost metric.

### 4.1 Architecture Search with Zero-cost Proxies

Our algorithm begins with an untrained supernet  $A_0$  which contains a set of edges  $\mathcal{E}$ , the number of searching iterations  $N$ , and the number of validation iterations  $V$ . In each searching iteration  $i$ , we start discretizing the supernet  $A_0$  using one of the possible edge orderings (more on that later). When discretizing each edge, we decide on the operation to use by using our proposed zero-cost-based

Table 2: Test error (%) of Zero-Cost-PT when using different search orders on NAS-Bench-201.

Search Order <sup>1</sup>	# of Perturbations <sup>2</sup>	C10	C100	ImageNet-16
fixed	$ \mathcal{O}  \mathcal{E} $	$5.98 \pm 0.50$	$27.60 \pm 1.63$	$54.23 \pm 0.93$
global-op-iter	$\frac{1}{2} \mathcal{O}  \mathcal{E} ( \mathcal{E}  + 1)$	$5.69 \pm 0.19$	$26.80 \pm 0.51$	$53.64 \pm 0.40$
global-op-once	$2 \mathcal{O}  \mathcal{E}  -  \mathcal{O} $	$6.30 \pm 0.57$	$28.96 \pm 1.66$	$55.04 \pm 1.47$
global-edge-iter	$\frac{1}{2} \mathcal{O}  \mathcal{E} ( \mathcal{E}  + 1)$	$6.23 \pm 0.45$	$28.42 \pm 0.59$	$54.39 \pm 0.47$
global-edge-once	$2 \mathcal{O}  \mathcal{E}  -  \mathcal{O} $	$6.30 \pm 0.57$	$28.96 \pm 1.66$	$55.04 \pm 1.47$
random	$ \mathcal{O}  \mathcal{E} $	$5.97 \pm 0.17$	$27.47 \pm 0.28$	$53.82 \pm 0.77$

<sup>1</sup> All methods use `nwo` metric,  $N=10$  search iterations and  $V=100$  validation iteration.

<sup>2</sup> Number of perturbations per search iteration.

perturbation function  $f_{zc-pt}$  which was able to achieve promising results in the preliminary experiments presented in the previous section. After all edges have been discretized, the final architecture is added to the set of candidates and we begin the process again for  $i + 1$  starting with the original  $A_0$ .

After all  $N$  candidate architectures have been constructed, the second stage begins. We score the candidate architectures again using a selected zero-cost metric (the same which is used in  $f_{zc-pt}$ ), but this time computing their end-to-end score rather than using the perturbation paradigm. We calculate the zero-cost metric for each network using  $V$  different minibatches of data. The final architecture is the architecture that achieves the best total score during the second stage. The full algorithm is outlined as Algorithm 1.

Our algorithm contains four main hyperparameters:  $N$ ,  $V$ , ordering of edges to follow when discretizing, and the zero-cost metric to use ( $S$ ). In the remaining of this section we present detailed ablation study which we performed to decide on the best possible configuration of these.

## 4.2 Ablation Study on NAS-Bench-201

We conduct a ablations of the proposed Zero-Cost-PT approach on NAS-Bench-201 [34]. NAS-Bench-201 constructed a unified cell-based search space, where each architecture has been trained on three different datasets, CIFAR-10, CIFAR-100 and ImageNet-16-120<sup>3</sup>. In our experiments, we take a randomly initialised supernet for this search space and apply our Zero-Cost-PT algorithm to search for architectures without any training. We run the search with four different random seeds (0, 1, 2, 3) and report the average and standard deviation of the test errors of the obtained architectures. All searches were performed on CIFAR-10, and obtained architectures were then additionally evaluated on the other two datasets.

**Edge Discretization Order.** We first study how different edge discretization order may impact the performance of our Zero-Cost-PT approach. We consider the following edge discretization orders:

- **fixed**: discretizes the edges in a fixed order, where in our experiments we discretize from the input towards the output of the cell structure;
- **random**: discretizes the edges in a random order (DARTS-PT);
- **global-op-iter**: iteratively evaluates  $S(A - (e, o))$  for all operations on all edges in  $\mathcal{E}$ , selects the edge  $e$  containing the operation  $o^*$  with globally best score. Discretizes  $e$  with  $o^*$ , then repeat the process to decide on the next edge (involves re-evaluation of scores) until all edges have been discretized;
- **global-op-once**: only evaluates  $S(A - (e, o))$  for all operations once to obtain a ranking order of the operations, and discretizes the edges  $\mathcal{E}$  according to this order;
- **global-edge-iter**: similar to **global-op-iter** but iteratively selects edge  $e$  from  $\mathcal{E}$  based on the average score of all operations on each edge;
- **global-edge-once**: similar to **global-op-once** but uses the average score of operations on edges to obtain the edge discretization order.

In our experiments we run  $N = 10$  search iterations and  $V = 100$  validation iterations for all variants. Table. 2 shows the performance of the approaches. We see that the **global-op-iter** consistently performs best across all three datasets, since it iteratively explores the search space of remaining operations, aiming to select the currently best in a greedy way. It also comes with a higher cost than **fixed** or **random**, since it needs to perturb  $\frac{1}{2}|\mathcal{O}||\mathcal{E}|(|\mathcal{E}| + 1)$  operations in total, while the latter

<sup>3</sup>We use the three random seeds available in NAS-Bench-201: 777, 888, 999.

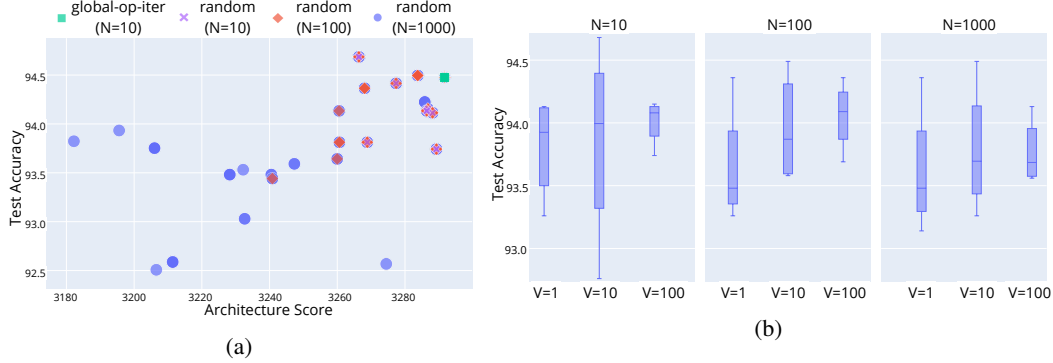


Figure 3: (a) Accuracy vs. score of architectures discovered on C10 by Zero-Cost-PT with different N. (b) Accuracy distribution of discovered architectures with different N and V.

require  $|\mathcal{O}||\mathcal{E}|$  ( $|\mathcal{E}|$  is the number of edges in the cell and  $|\mathcal{O}|$  is the number of operations on each edge). On the other hand, we see that although cheaper, the performance of `global-op-once` is inferior since it determines the order to perturb edges by assessing the importance of operations once for all at the beginning, which may not be appropriate as discretization continues. Note that when discretizing an edge according to the obtained order, `global-op-once` still need to perturb the  $|\mathcal{O}|$  operations on each remaining edge. We observe similar behaviour in `global-edge-iter` and `global-edge-once`, both of which use the average importance of operations on edges to decide search order, leading to suboptimal performance. It is also worth pointing out that `fixed` performs relatively well comparing to the other variants, offering comparable performance with `random`. This shows that Zero-Cost-PT is generally robust to the edge discretization order. For simplicity, in the following experiments we use `random` order with a moderate setting in search iterations ( $N = 10$ ) to balance exploration and exploitation during search, while maintaining the efficiency of Zero-Cost-PT.

**Search vs. Validation.** We also study the impact of different search iterations  $N$  and validation iterations  $V$  when our Zero-Cost-PT use `random` as the search order. Intuitively, larger  $N$  lead to more architecture candidates being found, while  $V$  indicates the amount of data used to rank the search candidates. As shown in Figure 3a, we see larger  $N$  does lead to more architectures discovered, but not proportional to the value of  $N$  on NAS-Bench-201 space. Notably for  $N=100$  we discover 27.8 distinct architectures on average, but when increased to  $N=1000$  the number only roughly doubles. We also see that even with  $N=10$ , Zero-Cost-PT (both `random` and `global-edge-iter`) can already discover top models in the space, demonstrating desirable balance between search quality and efficiency. On the other hand, as shown in Figure 3b, larger  $V$  tends to reduce the performance variance, especially for smaller  $N$ . This is also expected as more validation iterations could stabilise the ranking of selected architecture candidates, helping Zero-Cost-PT to retain the most promising ones at manageable cost ( $V$  minibatches of data).

**Different Zero-cost Metrics.** We empirically investigate the performance of our Zero-Cost-PT algorithm when using different zero-cost metrics. In particular, we consider the following metrics that have been proposed in recent zero-cost NAS literature [16, 17]: `grad_norm` [16], `snip` [29], `grasp` [28], `synflow` [27], `fisher` [35] and `nwot` [17]. Table 3 compares the average test errors of architectures selected by different proxies on NAS-Bench-201. We see that `nwot` and `synflow` perform considerably better across the three datasets than the others, where `nwot` offers around 0.27% improvement over `synflow`. However, even the worst performing `fisher` and naive `grad_norm` outperform the state-of-the-art DARTS-PT on this benchmark (see Table 4). This confirms that the zero-cost metrics, when combined with the perturbation-based NAS paradigms as in Zero-Cost-PT, could become promising proxies to the actual trained accuracy. We also observed that the ranking of those metrics are quite stable on the three datasets (descending order in terms

Table 3: Test error (%) of Zero-Cost-PT with different proxies on NAS-Bench-201.

Proxy <sup>1</sup>	CIFAR-10	CIFAR-100	ImageNet-16
<code>fisher</code>	$10.64 \pm 1.27$	$38.48 \pm 1.96$	$82.85 \pm 12.63$
<code>grad_norm</code>	$10.55 \pm 1.11$	$38.43 \pm 2.10$	$80.71 \pm 12.10$
<code>grasp</code>	$9.81 \pm 3.42$	$36.52 \pm 6.33$	$64.27 \pm 8.82$
<code>snip</code>	$8.32 \pm 2.02$	$34.00 \pm 4.03$	$65.35 \pm 11.04$
<code>synflow</code> <sup>2</sup>	$6.24 \pm 0.00$	$28.89 \pm 0.00$	$58.56 \pm 0.00$
<code>nwot</code>	$5.97 \pm 0.17$	$27.47 \pm 0.28$	$53.82 \pm 0.77$

<sup>1</sup> All proxies use  $N=10$  search iterations and  $V=100$  validation iteration.

<sup>2</sup> Only 1 model was selected across all 4 seeds.

of error as in Table 3), indicating that architectures discovered by our Zero-Cost-PT have good transferability across datasets. It is also clear that `nwot` consistently performs the best, reducing test errors on all three datasets by a considerable margin.

## 5 Results

In the previous section we introduced our Zero-Cost-PT method and performed some ablation studies on NAS-Bench-201 [34] to find the best performing set of hyperparameters. In this section we further compare the proposed Zero-Cost-PT approach with the state-of-the-art zero-cost and perturbation based NAS algorithms on a number of search spaces, including NAS-Bench-201 [34], DARTS’ CNN space [12] and the four DARTS subspaces S1-S4 [13]. We use the same setting as in Section 4.2, and details can be found in supplementary materials (S.M.).

### 5.1 Comparison with SOTA on NAS-Bench-201

Table. 4 shows the average test error (%) of the competing approaches and our Zero-Cost-PT on the three datasets in NAS-Bench-201. Here we include the naive random search and original DARTS as baselines, and compare our approach with the recent zero-cost NAS algorithm NASWOT [17], as well as the perturbation-based NAS approaches DARTS-PT and DARTS-PT (fix  $\alpha$ ) [33]. As in all competing approaches, we perform search on CIFAR-10 and evaluate the final model on all three datasets. We see that on all datasets our Zero-Cost-PT consistently offers superior performance, especially on CIFAR-100 and ImageNet-16. We see that even the best perturbation-based algorithm, DARTS-PT (fix  $\alpha$ ), fails on those two datasets, producing suboptimal results with limited improvements compared to random search. This suggests that architectures discovered by DARTS-PT might not transfer well to other datasets. On the other hand our Zero-Cost-PT can discover architectures that consistently perform well even after transferring to a different dataset – especially when used with `nwot` metric.

### 5.2 Results on DARTS CNN Search Space

We now move to the much larger DARTS CNN search spaces. We compare the proposed Zero-Cost-PT with the original DARTS and its variants, as well as the recent perturbation-based DARTS-PT [33]. We use the same settings as in DARTS-PT [33], but instead of pre-training the supernet and fine-tuning it after each perturbation, we take an untrained supernet and directly perform zero-cost perturbation-based architecture search as in Algorithm 1. As in previous experiments, we run our Zero-Cost-PT algorithm with  $N=10$  search iterations and  $V=100$  validation iteration, using the same random seeds as in DARTS-PT. We then train the selected four

Table 4: Comparison in test error (%) with the state-of-the-art perturbation-based and zero-cost NAS on NAS-Bench-201.

Method	CIFAR-10	CIFAR-100	ImageNet-16
Random	$13.39 \pm 13.28$	$39.17 \pm 12.58$	$66.87 \pm 9.66$
DARTS [12]	$45.70 \pm 0.00$	$84.39 \pm 0.00$	$83.68 \pm 0.00$
DARTS-PT [33] <sup>1</sup>	$11.89 \pm 0.00$	$45.72 \pm 6.26$	$69.60 \pm 4.40$
DARTS-PT (fix $\alpha$ ) [33] <sup>1</sup>	$6.20 \pm 0.00$	$34.03 \pm 2.24$	$61.36 \pm 1.91$
NASWOT(synflow) [16] <sup>2</sup>	$6.54 \pm 0.62$	$29.53 \pm 2.13$	$58.22 \pm 4.18$
NASWOT(nwot) [17] <sup>2</sup>	$7.04 \pm 0.80$	$29.97 \pm 1.16$	$55.57 \pm 2.07$
Zero-Cost-PT(synflow)	$6.24 \pm 0.00$	$28.89 \pm 0.00$	$58.56 \pm 0.00$
Zero-Cost-PT(nwot)	$5.97 \pm 0.17$	$27.47 \pm 0.28$	$53.82 \pm 0.77$

<sup>1</sup> Results on C10 taken from [33]. Results on other datasets computed using official code in [33], and averaged over results using 4 random seeds (0 - 3).

<sup>2</sup> Calculated with  $N=1000$  and averaged over 500 runs as described in [17].

Table 5: Comparison with the state-of-the-art differentiable NAS methods on the DARTS CNN search space (CIFAR-10).

Method	Test Error (%)		Params (M)	Cost <sup>2</sup>
	Avg.	Best		
DARTS [12]	$3.00 \pm 0.14$	-	3.3	0.4
SDARTS-RS [31]	$2.67 \pm 0.03$	-	3.4	0.4
SGAS [32]	$2.66 \pm 0.24$	-	3.7	0.25
DARTS+PT [33]	$2.61 \pm 0.08$	$2.48$	3.0	0.8
DARTS+PT <sub>none</sub> <sup>1</sup>	$2.73 \pm 0.13$	2.67	3.2	0.8
Zero-Cost-PT <sub>random</sub>	$2.68 \pm 0.17$	$2.43$	4.7	$0.018$
Zero-Cost-PT <sub>global-op-iter</sub>	$2.62 \pm 0.09$	2.49	4.6	$0.17$

<sup>1</sup> `none` operation muted in code provided by DARTS+PT [33]. Results obtained by re-enabling `none` in search.

<sup>2</sup> In GPU days. Cost of existing approaches taken from [33]. Cost of Zero-Cost-PT measured on a single 2080Ti GPU.

architectures under different initialisation (seeds 0-3) for 600 epochs, and report both the best and average test errors on CIFAR-10. Training details can be found the in S.M.

As shown in Table 5 the proposed Zero-Cost-PT approaches can achieve much better average test error than the original DARTS and comparable to its newer variants SDARTS-RS [31] and SGAS [32] at a much lower searching cost (especially when using random edge ordering). The significant improvement over DARTS+PT comes from the fact that DARTS-PT needs to compute validation accuracy of the supernet after each operation perturbed (removed), where the remaining supernet requires extra fine-tuning to recover from accuracy drop between two perturbations. On the other hand in our Zero-Cost-PT<sub>random</sub>, we only need to evaluate the score of the perturbed supernet with zero-cost proxies (in these experiments we use  $S_{\text{nwot}}$ ), requiring no more than a minibatch of data. Note that here the cost of Zero-Cost-PT reported in Table 5 is for N=10 search iterations (randomly selecting the order of edges to perturb in each iteration), and thus a single search iteration only takes about a few minutes to run. The other variant Zero-Cost-PT<sub>global-op-iter</sub>, which uses global-op-iter to determine edge discretization order (see Section 4.2), offers better performance with lower variance compared to random but incurs slightly heavier computation.

### 5.3 Results on DARTS Spaces S1-S4

As described in the previous sections, it is well known that DARTS could generate trivial architectures with degenerative performance in certain cases. Zela et al. [13] have designed various special search spaces for DARTS in order to investigate its failure cases on them. As in DARTS+PT, we consider spaces S1-S4 and study the performance of our Zero-Cost-PT on them to validate its robustness in a controlled environment. Detailed specifications of S1-S4 can be found in the S.M.

As shown in Table 6, our approach consistently outperforms the original DARTS, the state-of-the-art DARTS-PT and DARTS-PT(fix  $\alpha$ ) across S1 to S3 on both datasets C10 and C100, while on SVHN it offers competitive performance comparing the competing algorithms (best in S1, second best in space S2/S3 with .08/.02% gap). This confirms that our Zero-Cost-PT is robust in finding good performing architectures in spaces where DARTS typically fails, e.g. it has been shown [33] that in S2 DARTS tends to produce trivial architectures saturated with skip connections. On the other hand, we observe that Zero-Cost-PT doesn't perform well in search space S4. In particular, our approach struggles with operation `noise`, which simply outputs a random Gaussian noise  $\mathcal{N}(0, 1)$  regardless of the input. This leads to unpredictable behaviour when our approach assesses the importance of this operation, i.e., the score  $S(\mathcal{A}_{\setminus o})$  can be completely random when  $o = \text{noise}$ . Therefore it is expected for our Zero-Cost-PT approach which involves no training in architecture search, to generate suboptimal results in this spaces.

## 6 Conclusion

In this paper, we propose Zero-Cost-PT, a perturbation-based NAS that utilises zero-cost proxies in the context of differentiable NAS. We shows that lightweight operation scoring methods based on zero-cost metrics empirically outperform existing operation scoring functions such as darts [12] and darts-pt [33]. We then presented a lightweight NAS algorithm based on perturbation and the zero-cost metrics. Our approach outperforms the best available differentiable architecture search in terms of searching time and accuracy even in very large search spaces – something that was previously impossible to achieve by using zero-cost proxies.

Table 6: Comparison in test error (%) with state-of-the-art perturbation-based NAS on DARTS spaces S1-S4 (best in red, 2nd best in blue).

Space	DARTS <sup>1</sup>		DARTS-PT <sup>1</sup>		Zero-Cost-PT <sup>2</sup>	
	Best	Best	Best (fix $\alpha$ )	Avg.	Best	
<b>CIFAR-10</b>						
S1	3.84	3.5	<b>2.86</b>	<b>2.75</b> $\pm$ 0.28	<b>2.55</b>	
S2	4.85	2.79	<b>2.59</b>	<b>2.49</b> $\pm$ 0.05	<b>2.45</b>	
S3	3.34	<b>2.49</b>	2.52	<b>2.47</b> $\pm$ 0.09	<b>2.40</b>	
S4	7.20	<b>2.64</b>	<b>2.58</b>	5.23 $\pm$ 0.76	4.69	
<b>CIFAR-100</b>						
S1	29.64	24.48	<b>24.4</b>	<b>22.05</b> $\pm$ 0.29	<b>21.84</b>	
S2	26.05	<b>23.16</b>	23.3	<b>20.97</b> $\pm$ 0.50	<b>20.61</b>	
S3	28.9	22.03	<b>21.94</b>	<b>21.02</b> $\pm$ 0.57	<b>20.61</b>	
S4	22.85	<b>20.80</b>	<b>20.66</b>	25.70 $\pm$ 0.01	25.69	
<b>SVHN</b>						
S1	4.58	2.62	<b>2.39</b>	<b>2.37</b> $\pm$ 0.06	<b>2.33</b>	
S2	3.53	2.53	<b>2.32</b>	<b>2.40</b> $\pm$ 0.05	<b>2.36</b>	
S3	3.41	2.42	<b>2.32</b>	2.34 $\pm$ 0.05	<b>2.30</b>	
S4	3.05	<b>2.42</b>	<b>2.39</b>	2.83 $\pm$ 0.06	2.79	

<sup>1</sup> Results taken from [33].

<sup>2</sup> Results obtained using random seeds 0 and 2.

## References

- [1] Forrest N. Iandola, Song Han, Matthew W. Moskewicz, Khalid Ashraf, William J. Dally, and Kurt Keutzer. SqueezeNet: Alexnet-level accuracy with 50x fewer parameters and <0.5mb model size. *arXiv:1602.07360*, 2016.
- [2] Andrew G. Howard, Menglong Zhu, Bo Chen, Dmitry Kalenichenko, Weijun Wang, Tobias Weyand, Marco Andreetto, and Hartwig Adam. MobileNets: Efficient Convolutional Neural Networks for Mobile Vision Applications. *arXiv preprint arXiv:1704.04861*, 2017.
- [3] Mingxing Tan and Quoc Le. EfficientNet: Rethinking model scaling for convolutional neural networks. In *International Conference on Machine Learning (ICML)*, 2019.
- [4] Mark Sandler, Andrew Howard, Menglong Zhu, Andrey Zhmoginov, and Liang-Chieh Chen. Mobilenetv2: Inverted residuals and linear bottlenecks. In *Proceedings of the IEEE/CVF Conference on Computer Vision and Pattern Recognition (CVPR)*, pages 4510–4520, 2018.
- [5] Mingxing Tan and Quoc V. Le. Efficientnetv2: Smaller models and faster training. *arXiv:2104.00298*, 2021.
- [6] Esteban Real, Alok Aggarwal, Yanping Huang, and Quoc V. Le. Regularized Evolution for Image Classifier Architecture Search. In *AAAI Conference on Artificial Intelligence (AAAI)*, 2019.
- [7] Bichen Wu, Xiaoliang Dai, Peizhao Zhang, Yanghan Wang, Fei Sun, Yiming Wu, Yuandong Tian, Peter Vajda, Yangqing Jia, and Kurt Keutzer. Fbnet: Hardware-aware efficient convnet design via differentiable neural architecture search. In *Proceedings of the IEEE/CVF Conference on Computer Vision and Pattern Recognition (CVPR)*, pages 10726–10734, 2019.
- [8] Han Cai, Chuang Gan, Tianzhe Wang, Zhekai Zhang, and Song Han. Once for all: Train one network and specialize it for efficient deployment. In *International Conference on Learning Representations (ICLR)*, 2020.
- [9] Bert Moons, Parham Noorzad, Andrii Skliar, Giovanni Mariani, Dushyant Mehta, Chris Lott, and Tijmen Blankevoort. Distilling optimal neural networks: Rapid search in diverse spaces. *arXiv:2012.08859*, 2020.
- [10] Renqian Luo, Fei Tian, Tao Qin, Enhong Chen, and Tie-Yan Liu. Neural architecture optimization. In *Proceedings of the 32nd International Conference on Neural Information Processing Systems, NIPS’18*, page 7827–7838, Red Hook, NY, USA, 2018. Curran Associates Inc.
- [11] Łukasz Dudziak, Thomas Chau, Mohamed S. Abdelfattah, Royson Lee, Hyeji Kim, and Nicholas D. Lane. BRP-NAS: Prediction-based NAS using GCNs. In *Neural Information Processing Systems (NeurIPS)*, 2020.
- [12] Hanxiao Liu, Karen Simonyan, and Yiming Yang. DARTS: Differentiable architecture search. In *International Conference on Learning Representations (ICLR)*, 2019.
- [13] Arber Zela, Thomas Elsken, Tonmoy Saikia, Yassine Marrakchi, Thomas Brox, and Frank Hutter. Understanding and robustifying differentiable architecture search. In *International Conference on Learning Representations (ICLR)*, volume 3, page 7, 2020.
- [14] Yao Shu, Wei Wang, and Shaofeng Cai. Understanding architectures learnt by cell-based neural architecture search. In *International Conference on Learning Representations*, 2020.
- [15] Kaicheng Yu, Christian Sciuto, Martin Jaggi, and Mathieu Salzmann Claudiu Musat. Evaluating the search phase of neural architecture search. In *International Conference on Learning Representations*, 2020.
- [16] Mohamed S Abdelfattah, Abhinav Mehrotra, Łukasz Dudziak, and Nicholas Donald Lane. Zero-cost proxies for lightweight NAS. In *International Conference on Learning Representations (ICLR)*, 2021.
- [17] Joseph Mellor, Jack Turner, Amos Storkey, and Elliot J. Crowley. Neural architecture search without training. In *International Conference on Machine Learning (ICML)*, 2021 (to appear).
- [18] Barret Zoph and Quoc V. Le. Neural architecture search with reinforcement learning. In *International Conference on Learning Representations (ICLR)*, 2017.
- [19] Hieu Pham, Melody Guan, Barret Zoph, Quoc Le, and Jeff Dean. Efficient neural architecture search via parameters sharing. In *International Conference on Machine Learning (ICML)*, pages 4095–4104, 2018.

[20] Gabriel Bender, Hanxiao Liu, Bo Chen, Grace Chu, Shuyang Cheng, Pieter-Jan Kindermans, and Quoc V. Le. Can weight sharing outperform random architecture search? an investigation with tunas. In *Proceedings of the IEEE/CVF Conference on Computer Vision and Pattern Recognition (CVPR)*, 2020.

[21] Royson Lee, Łukasz Dudziak, Mohamed Abdelfattah, Stylianos I. Venieris, Hyeji Kim, Hongkai Wen, and Nicholas D. Lane. Journey towards tiny perceptual super-resolution. In *European Conference on Computer Vision (ECCV)*, 2020.

[22] Dongzhan Zhou, Xinchi Zhou, Wenwei Zhang, Chen Change Loy, Shuai Yi, Xuesen Zhang, and Wanli Ouyang. Econas: Finding proxies for economical neural architecture search. In *Proceedings of the IEEE/CVF Conference on Computer Vision and Pattern Recognition (CVPR)*, 2020.

[23] Abhinav Mehrotra, Alberto Gil Ramos, Sourav Bhattacharya, Łukasz Dudziak, Ravichander Vipperla, Thomas Chau, Mohamed S. Abdelfattah, Samin Ishtiaq, and Nicholas D. Lane. NAS-Bench-ASR: Reproducible Neural Architecture Search for Speech Recognition. In *International Conference on Learning Representations (ICLR)*, 2021.

[24] Chen Wei, Chuang Niu, Yiping Tang, and Ji min Liang. Npenas: Neural predictor guided evolution for neural architecture search. *arXiv:2003.12857*, 2020.

[25] Junru Wu, Xiyang Dai, Dongdong Chen, Yinpeng Chen, Mengchen Liu, Ye Yu, Zhangyang Wang, Zicheng Liu, Mei Chen, and Lu Yuan. Weak NAS predictors are all you need. *arXiv:2102.10490*, 2021.

[26] Wei Wen, Hanxiao Liu, Hai Li, Yiran Chen, Gabriel Bender, and Pieter-Jan Kindermans. Neural predictor for neural architecture search. *arXiv:1912.00848*, 2019.

[27] Hidenori Tanaka, Daniel Kunin, Daniel L. K. Yamins, and Surya Ganguli. Pruning neural networks without any data by iteratively conserving synaptic flow. In *Neural Information Processing Systems (NeurIPS)*, 2020.

[28] Chaoqi Wang, Guodong Zhang, and Roger Grosse. Picking winning tickets before training by preserving gradient flow. In *International Conference on Learning Representations (ICLR)*, 2020.

[29] Namhoon Lee, Thalaiyasingam Ajanthan, and Philip HS Torr. Snip: Single-shot network pruning based on connection sensitivity. In *International Conference on Learning Representations (ICLR)*, 2019.

[30] Jack Turner, Elliot J. Crowley, Michael O’Boyle, Amos Storkey, and Gavin Gray. Block-swap: Fisher-guided block substitution for network compression on a budget. In *International Conference on Learning Representations (ICLR)*, 2020.

[31] Xiangning Chen and Cho-Jui Hsieh. Stabilizing differentiable architecture search via perturbation-based regularization. In *International Conference on Machine Learning (ICML)*, pages 1554–1565. PMLR, 2020.

[32] Guohao Li, Guocheng Qian, Itzel C Delgadillo, Matthias Muller, Ali Thabet, and Bernard Ghanem. Sgas: Sequential greedy architecture search. In *Proceedings of the IEEE/CVF Conference on Computer Vision and Pattern Recognition (CVPR)*, pages 1620–1630, 2020.

[33] Ruochen Wang, Minhao Cheng, Xiangning Chen, Xiaocheng Tang, and Cho-Jui Hsieh. Re-thinking architecture selection in differentiable NAS. In *International Conference on Learning Representations (ICLR)*, 2021.

[34] Xuanyi Dong and Yi Yang. NAS-Bench-201: Extending the Scope of Reproducible Neural Architecture Search. In *International Conference on Learning Representations (ICLR)*, 2020.

[35] Lucas Theis, Iryna Korshunova, Alykhan Tejani, and Ferenc Huszár. Faster gaze prediction with dense networks and fisher pruning. *arXiv:1801.05787*, 2018.

[36] Yuhui Xu, Lingxi Xie, Xiaopeng Zhang, Xin Chen, Guo-Jun Qi, Qi Tian, and Hongkai Xiong. Pcdarts: Partial channel connections for memory-efficient architecture search. In *International Conference on Learning Representations*, 2020.

## A Appendix

### A.1 More on Operation Scoring

In this section, we provide more experimental details and results of our analysis of the operation scoring functions introduced in Section 3. Most notably, we empirically study these functions in the *iterative* setting.

#### A.1.1 Iterative Operation Selection

One major finding from Figure 2 is that discretization accuracy does not represent the true operation strength at all, in fact, in our experiments it was negatively-correlated with best-acc (which is the ideal scoring function). Another interesting finding is that zero-cost based methods, especially zc-pt, performed very well, even outperforming the recently-introduced darts-pt [33]. However, one shortcoming of our analysis and conclusions in Section 3 is that we only consider operation scores at iteration 0, whereas most of the operation scoring functions are meant to be used within an iterative algorithm: score  $\rightarrow$  discretize  $\rightarrow$  (optional) train  $\rightarrow$  score.

To investigate the correlation of scoring functions in the iterative setting, we do the following:

1. score operations on all undiscretized edges,
2. discretize edge  $i$ ,
3. retrain for 5 epochs (darts-pt and disc-acc only),
4. increment  $i$  and repeat from step 1 until all edges are discretized.

At each iteration  $i$ , we calculate the scores for the operations on all remaining undiscretized edges and compute their Spearman rank correlation coefficients (Spearman- $\rho$ ) w.r.t. best-acc. This is plotted in Figure A1, averaged over four seeds. Our results confirm many of our iteration-0 analysis. zc-pt continues to be the best operation scoring function, and darts-pt is the second-best. Additionally, disc-acc continues to be unrepresentative of operation strength even when used in the iterative setting. This is not what we expected, especially in the very last iteration when disc-acc is supposed to match a subnetwork exactly. As Figure A1 shows, the variance in the last iteration is quite large – we believe this happens because we do not train to convergence every time we discretize an edge, and instead we only train for 5 epochs. In future work (and possibly, in revisions of this manuscript) we will re-evaluate discretization accuracy with a larger number of retraining epochs. For now, our main conclusion regarding the disc-acc scoring function is that it is unrepresentative of true operation strength when we only use 5 epochs of retraining.

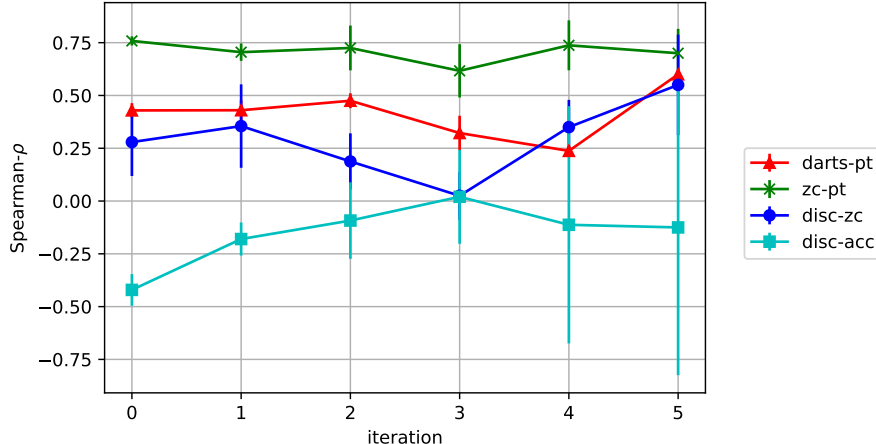


Figure A1: Rank correlation coefficient of operation scoring functions versus best-acc when invoked iteratively for each edge. In iteration  $i$ , only edge  $i$  is discretized then all scores for all operations on the remaining edges is computed and correlated against best-acc.

Table A1: Comparison to previous work on the ImageNet classification task. We performed our search using the CIFAR-10 dataset as described in Section 5, similarly to previous work.

Architecture	Test Error [%]		Params [MB]	Search Time [GPU-days]
	Top-1	Top-5		
DARTS [12]	26.7	8.7	4.7	0.4
SDARTS-RS [31]	25.6	8.2	-	0.4
DARTS-PT [33]	25.5	8.0	4.6	0.8
PC-DARTS [36]	25.1	7.8	5.3	0.1
SGAS [32]	24.1	7.3	5.4	0.25
Zero-Cost-PT <sup>1</sup> (best)	24.4	7.5	6.3	0.018
Zero-Cost-PT <sup>1</sup> (4 seeds)	24.6 $\pm$ 0.13	7.6 $\pm$ 0.09	6.3	0.018

<sup>1</sup> We use the same training pipeline from DARTS [12].

### A.1.2 Detailed Methodology

Here, we provide some additional experimental details for the data presented in Section 3. The following list describes how we compute each operation score.

- **best-acc**: To get the score for an operation  $o$  on a specific edge  $e$ , we find the maximum test accuracy of all NAS-Bench-201 architectures with  $(o, e)$ .
- **avg-acc**: Same as best-acc but we *average* all NAS-Bench-201 architecture test accuracies instead of finding the maximum.
- **disc-acc**: We discretize one edge  $e$  by selecting an operation  $o$ , then we train for 5 epochs<sup>4</sup> and record the supernet accuracy – this is used as the score for  $(o, e)$ .
- **darts-pt**: We perturb one edge with one operation  $A - (e, o)$  and record the validation accuracy. For perturbation-based scoring functions, we multiply the score by  $-1$  before computing correlations.
- **disc-zc**: We discretize one edge  $e$  by selecting an operation  $o$  and then compute the zero-cost metric.
- **zc-pt**: We perturb one edge with one operation  $A - (e, o)$  and compute the zero-cost metric. For perturbation-based scoring functions, we multiply the score by  $-1$  before computing correlations.
- **darts**: We record the value of the architecture parameters  $\alpha$  after 60 epochs of training the supernet.

### A.1.3 Detailed Operation Scores

Table A2 (at the end of this Appendix) shows all operation scores at iteration 0. This data was used to compute Spearman- $\rho$  in Figure 2. Note that we compute Spearman- $\rho$  per edge, and average over all edges – this summarizes how well each score tracks our “oracle” best-acc score.

## A.2 Evaluation on ImageNet

Table A1 shows the ImageNet classification accuracy for architectures searched on CIFAR-10. Our Zero-Cost-PT<sub>random</sub> algorithm (from Table 5) is able to find architectures with a comparable accuracy much faster than previous work.

### A.3 Description of DARTS subspaces (S1-S4)

RobustDARTS introduced four different DARTS subspaces to evaluate robustness of the original DARTS algorithm [13]. In our work we validate robustness of Zero-Cost-PT against some of the more recent algorithms using the same subspaces originally proposed in the RobustDARTS paper (Section 5.3). The search spaces are defined as follows:

<sup>4</sup>DARTS-PT defines discretization accuracy as the accuracy after *convergence*. We elected to only train for 5 epochs to make our experiments feasible but we are now investigating whether longer training will affect our results.

---

**Algorithm 2:** Zero-Cost Perturbation-based Architecture Search (Zero-Cost-PT)

---

**Input :** An *untrained* supernet  $A_0$  with set of edges  $\mathcal{E}$  and set of nodes  $\mathcal{N}$ , # of search iterations  $N$ , # of validation iterations  $V$

**Result:** A selected architecture  $A_{|\mathcal{E}|}^*$

// Stage 1: search for architecture candidates

1  $\mathcal{C} = \emptyset$

2 **for**  $i = 1 : N$  **do**

3   **for**  $t = 1 : |\mathcal{E}|$  **do**

4     Select next edge  $e_t$  using the chosen discretization ordering

5      $o_t = f_{zc-pt}(A_{t-1}, e_t)$

6      $A_t = A_{t-1} + (e_t, o_t)$

7   **end**

8   **while**  $|\mathcal{N}| > 0$  **do** // prune the edges of the obtained architecture  $A_{|\mathcal{E}|}$

9     Randomly select a node  $n \in \mathcal{N}$

10    **forall** Input edge  $e$  to node  $n$  **do**

11     | Evaluate the zc-pt score of the architecture  $A_{|\mathcal{E}|}$  when  $e$  is removed

12    **end**

13     Retain only edges  $e_n^{(1)*}, e_n^{(2)*}$  with the 1st and 2nd best zc-pt score, and remove  $n$  from  $\mathcal{N}$

14   **end**

15   Add  $A_{|\mathcal{E}|}$  to the set of candidate architectures  $\mathcal{C}$

16 **end**

// Stage 2: Validate the architecture candidates

17 **for**  $j = 1 : V$  **do**

18   | Calculate  $S^{(j)}(A)$  for each  $A \in \mathcal{C}$  using a random mini-batch data;

19 **end**

20 Select the best architecture  $A_{|\mathcal{E}|}^* = \arg \max_{A \in \mathcal{C}} \sum_{j=1:V} S^{(j)}(A)$ ;

---

- in S1 each edge of a supernet consists only of the two candidate operations having the highest magnitude of  $\alpha$  in the vanilla DARTS (these operations can be different for different edges);
- S2 only considers two operations: `skip_connect` and `sep_conv_3x3`;
- similarly, S3 consists of three operations: `none`, `skip_connect` and `sep_conv_3x3`;
- finally, S4 again considers just two operation: `noise` and `sep_conv_3x3`, where `noise` operation generates random Gaussian noise  $\mathcal{N}(0, 1)$  in every forwards pass that is independent from the input.

#### A.4 Detailed Zero-Cost-PT Algorithm

For DARTS CNN search space, our Zero-Cost-PT algorithm has an additional topology selection step, where for each node in an architecture we only retain the top two incoming edges based on the zc-pt score – this is similar to the vanilla DARTS algorithm [12]. The detailed algorithms is presented in Algorithm 2.

#### A.5 Experimental Details

All searches were run multiple times with different searching seeds (usually 0, 1, 2 and 3). Additionally, each found architecture was trained multiple times using different training seeds – for DARTS the same set of seeds was used for training and searching, for NAS-Bench-201 (NB201) training seeds were taken from the dataset (777, 888 and 999, based on their availability in the dataset). Therefore, for each experiment we got a total of `searching_seeds`  $\times$  `training_seeds` accuracy values. Whenever average performance is reported, it was averaged across all obtained results. Similarly, best values were selected by taking the best single result from among the searching and training seeds.

##### A.5.1 Experimental Details – NAS-Bench-201

Searching was performed using 4 different seeds (0, 1, 2, and 3) to initialise a supernet. Whenever we had to perform training of a supernet during the searching phase (Section 3), we used the same

hyperparameters as used by the original DARTS-PT code. When searching using our Zero-Cost-PT we used batch size of 256,  $N=10$ ,  $V=100$  and  $S=nwot$ , unless mentioned otherwise (e.g., during ablation studies). Inputs for calculating zero-cost scores were coming from the training dataloader(s), as defined for relevant datasets in the original DARTS-PT code (including augmentation). For zero-cost proxies that require a loss function standard cross-entropy was used. For any searching method, after a final subnetwork had been identified by an algorithm, we extracted the final architecture and queried the NB201 dataset to obtain test accuracy – one value for each training seed available in the dataset.

All experiments specifically concerning operation scoring (Sections 3 and A.1) were using averaged accuracy of models from NB201 for simplicity.

We did not search for architectures targeting CIFAR-100 or ImageNet-16 directly – whenever we report results for these datasets we used the same architecture that had been found using CIFAR-10.

### A.5.2 Experimental Details – DARTS

DARTS experiments follow a similar methodology to NB201. Each algorithm was run with 4 different initialisation seeds for a supernet (0, 1, 2 and 3). When running Zero-Cost-PT, we used the following hyperparameters: batch size of 64,  $N=10$ ,  $V=100$  and  $S=nwot$ . Inputs and loss function for zero-cost metrics were defined analogically to NB201. We did not run any baseline method on the DARTS search space (all results were taken from the literature) so we did not have to perform any training of a supernet. After an algorithm had identified a final subnetwork, we then trained it 4 times using different initialisation seeds again (0, 1, 2 and 3). When training subnetworks we were using a setting aligned with the previous work [12, 33].

Unlike NB201, whenever different datasets were considered (Section 5.3) architectures were searched on each relevant dataset directly.

For CIFAR-10 experiments, we trained models using a heavy configuration with `init_channels=36` and `layers=20`. Models found on CIFAR-100 and SVHN were trained using a mobile setting with `init_channels=16` and `layers=8`. Both choices follow the previous work [13, 33].

### A.6 Discovered Architectures

Figures A2 and A3 present cells found by our Zero-Cost-PT on the DARTS CNN search space (Section 5.2) when using `global-op-iter` and `random` discretization orders, respectively (see Section 4.2 for the definition of the two discretization orders). Figures A4 through A15 show cells discovered on the four DARTS subspaces and the three relevant datasets (Sections 5.3 and A.3).

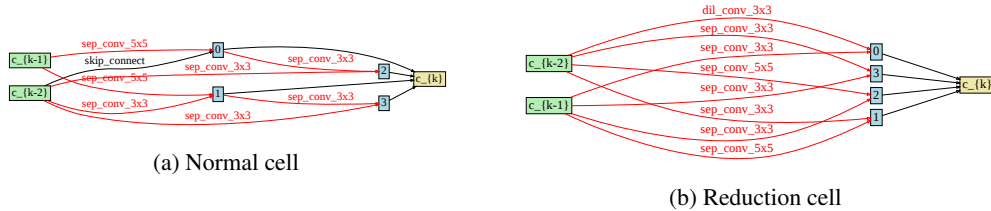


Figure A2: Cells found by Zero-Cost-PT (`global-op-iter` discretization order) on the DARTS search space using CIFAR-10.

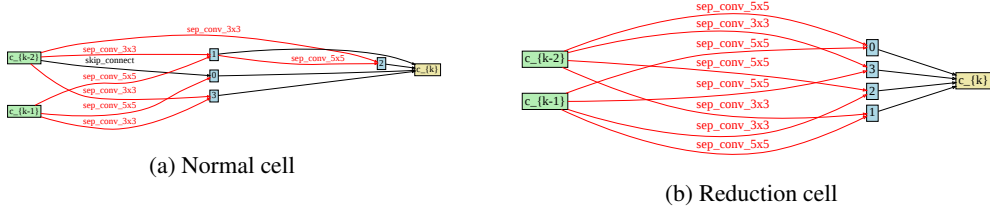


Figure A3: Cells found by Zero-Cost-PT (random discretization order) on the DARTS search space using CIFAR-10.

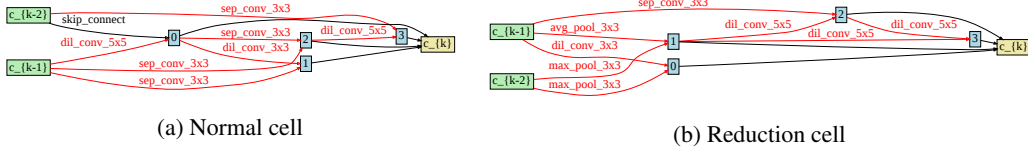


Figure A4: Cells found by Zero-Cost-PT (random discretization order) on the DARTS-S1 space using CIFAR-10.

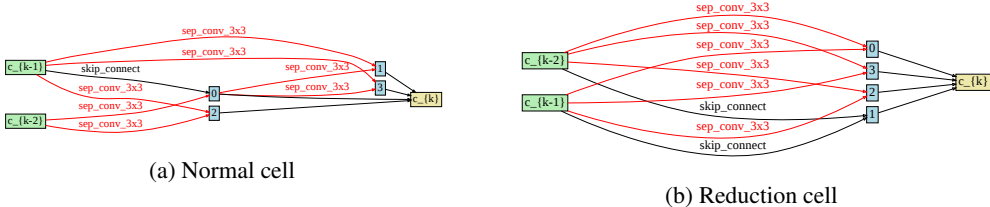


Figure A5: Cells found by Zero-Cost-PT (random discretization order) on the DARTS-S2 space using CIFAR-10.

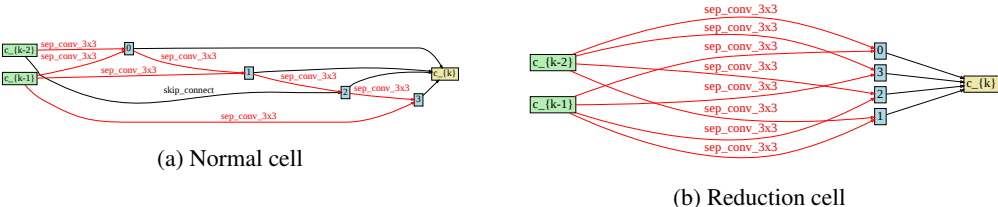


Figure A6: Cells found by Zero-Cost-PT (random discretization order) on the DARTS-S3 space using CIFAR-10.

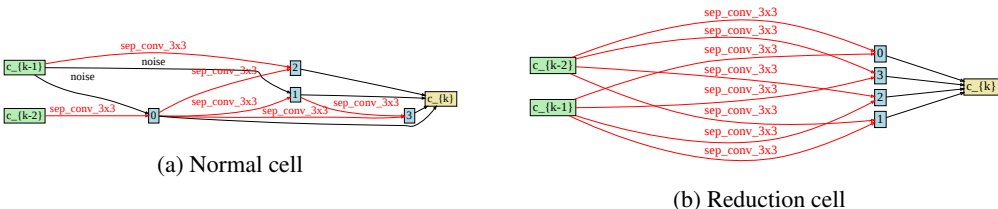


Figure A7: Cells found by Zero-Cost-PT (random discretization order) on the DARTS-S4 space using CIFAR-10.

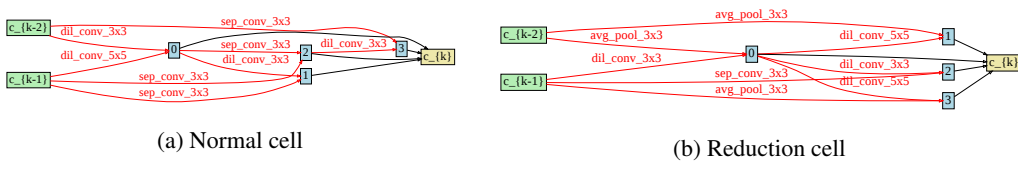


Figure A8: Cells found by Zero-Cost-PT (random discretization order) on the DARTS-S1 space using CIFAR-100.

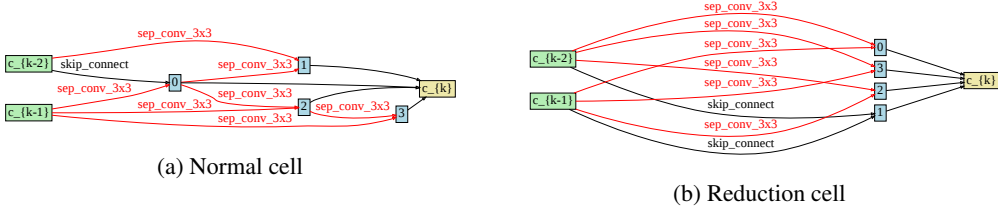


Figure A9: Cells found by Zero-Cost-PT (random discretization order) on the DARTS-S2 space using CIFAR-100.

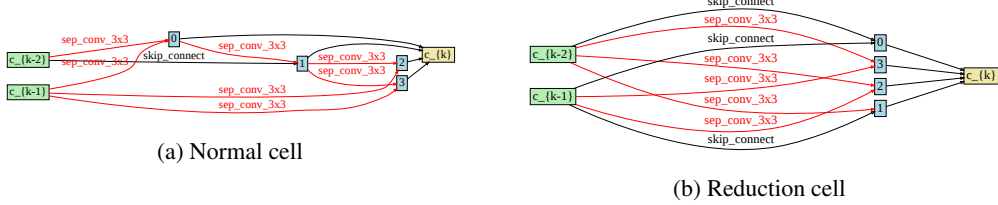


Figure A10: Cells found by Zero-Cost-PT (random discretization order) on the DARTS-S3 space using CIFAR-100.

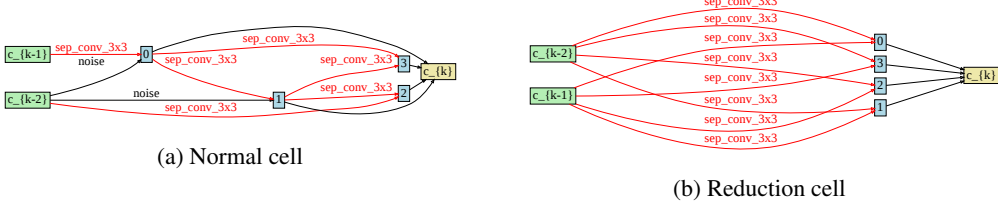


Figure A11: Cells found by Zero-Cost-PT (random discretization order) on the DARTS-S4 space using CIFAR-100.

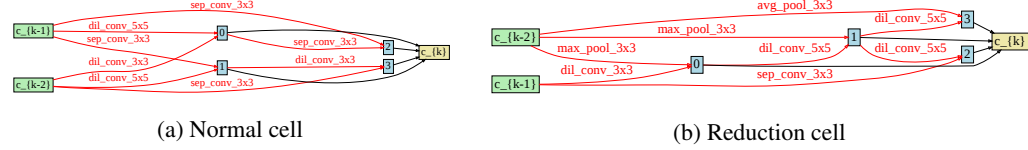


Figure A12: Cells found by Zero-Cost-PT (random discretization order) on the DARTS-S1 space using SVHN.

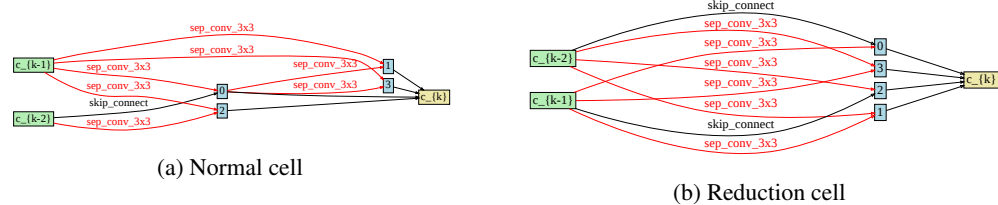


Figure A13: Cells found by Zero-Cost-PT (random discretization order) on the DARTS-S2 space using SVHN.

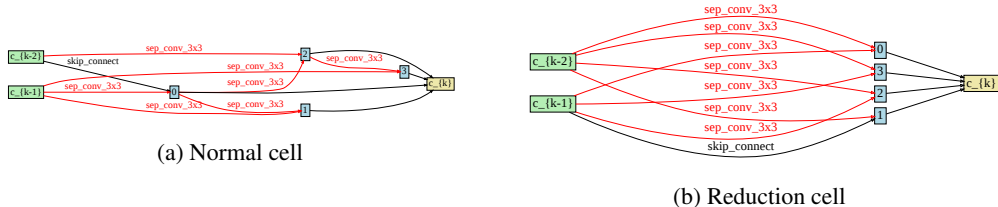


Figure A14: Cells found by Zero-Cost-PT (random discretization order) on the DARTS-S3 space using SVHN.

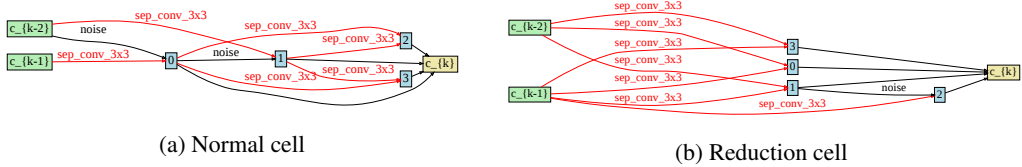


Figure A15: Cells found by Zero-Cost-PT (random discretization order) on the DARTS-S4 space using SVHN.

Table A2: Raw values of operation scoring functions at iteration 0 to reproduce Figure 2.

edge\op	none	skip_connect	nor_conv_1x1	nor_conv_3x3	avg_pool_3x3
best-acc	0	94.15	94.18	<b>94.44</b>	<b>94.68</b>
	1	94.24	94.16	<b>94.49</b>	<b>94.68</b>
	2	94.25	94.43	<b>94.49</b>	<b>94.68</b>
	3	<b>94.16</b>	<b>94.68</b>	94.03	94.04
	4	94.29	94.18	<b>94.56</b>	<b>94.68</b>
	5	94.05	94.16	<b>94.68</b>	<b>94.56</b>
avg-acc	0	77.36	81.02	83.81	<b>86.38</b>
	1	80.03	83.11	<b>85.23</b>	<b>85.99</b>
	2	82.9	82.44	<b>84.05</b>	<b>84.49</b>
	3	74.02	85.17	<b>87.3</b>	<b>88.28</b>
	4	80.14	83.05	<b>85.09</b>	<b>85.7</b>
	5	77.61	83.43	<b>86.18</b>	<b>86.95</b>
disc-acc	0	<b>83.27</b>	<b>82.24</b>	65.0	71.76
	1	<b>84.94</b>	83.23	73.23	76.77
	2	<b>83.87</b>	<b>83.73</b>	77.33	76.83
	3	65.77	<b>84.44</b>	75.82	<b>78.68</b>
	4	<b>83.57</b>	82.03	75.02	76.09
	5	<b>83.95</b>	<b>82.45</b>	66.69	71.36
darts-pt <sup>1</sup>	0	-85.43	<b>-17.02</b>	-78.13	<b>-59.09</b>
	1	-85.52	<b>-36.1</b>	-84.39	<b>-80.95</b>
	2	-85.51	<b>-80.29</b>	-81.86	<b>-77.68</b>
	3	-85.49	<b>-9.86</b>	-81.79	<b>-59.18</b>
	4	-85.45	<b>-51.15</b>	-78.84	<b>-64.64</b>
	5	-85.54	<b>-32.43</b>	-81.04	<b>-72.75</b>
disc-zc	0	3331.01	<b>3445.49</b>	3366.88	<b>3437.55</b>
	1	3429.07	<b>3435.75</b>	3407.87	<b>3434.58</b>
	2	3428.8	3423.36	<b>3440.93</b>	<b>3437.29</b>
	3	3408.99	<b>3464.05</b>	3359.89	3382.18
	4	<b>3433.99</b>	<b>3435.57</b>	3424.47	<b>3431.81</b>
	5	<b>3434.42</b>	<b>3437.66</b>	3418.57	3397.52
zc-pt <sup>1</sup>	0	-3455.23	-3449.9	<b>-3449.54</b>	<b>-3441.82</b>
	1	-3452.15	-3448.7	<b>-3441.81</b>	<b>-3440.65</b>
	2	-3446.52	-3447.61	<b>-3435.46</b>	<b>-3436.4</b>
	3	-3453.81	<b>-3435.99</b>	<b>-3444.04</b>	-3445.6
	4	-3451.06	-3449.8	<b>-3442.63</b>	<b>-3441.13</b>
	5	-3450.97	-3448.21	<b>-3440.8</b>	<b>-3443.24</b>
darts	0	0.14	<b>0.48</b>	0.13	<b>0.18</b>
	1	0.12	<b>0.55</b>	0.11	<b>0.12</b>
	2	<b>0.24</b>	<b>0.33</b>	0.15	0.17
	3	0.06	<b>0.65</b>	0.08	<b>0.13</b>
	4	0.12	<b>0.48</b>	0.13	<b>0.17</b>
	5	<b>0.16</b>	<b>0.49</b>	0.12	0.14

<sup>1</sup> Lower is better so we add a negative sign to \*-pt scores.